Mengyao Li,[1] Sara G. Vienberg,[1,2] Olivier Bezy,[1] Brian T. O'Neill,[1] and C. Ronald Kahn[1]

Role of PKCδ in Insulin Sensitivity and Skeletal Muscle Metabolism

Diabetes 2015;64:4023–4032 | DOI: 10.2337/db14-1891

Protein kinase C (PKC)δ has been shown to be increased in liver in obesity and plays an important role in the development of hepatic insulin resistance in both mice and humans. In the current study, we explored the role of PKCδ in skeletal muscle in the control of insulin sensitivity and glucose metabolism by generating mice in which PKCδ was deleted specifically in muscle using Cre-lox recombination. Deletion of PKCδ in muscle improved insulin signaling in young mice, especially at low insulin doses; however, this did not change glucose tolerance or insulin tolerance tests done with pharmacological levels of insulin. Likewise, in young mice, muscle-specific deletion of PKCδ did not rescue high-fat diet–induced insulin resistance or glucose intolerance. However, with an increase in age, PKCδ levels in muscle increased, and by 6 to 7 months of age, muscle-specific deletion of PKCδ improved whole-body insulin sensitivity and muscle insulin resistance and by 15 months of age improved the age-related decline in whole-body glucose tolerance. At 15 months of age, M-PKCδKO mice also exhibited decreased metabolic rate and lower levels of some proteins of the OXPHOS complex suggesting a role for PKCδ in the regulation of mitochondrial mass at older age. These data indicate an important role of PKCδ in the regulation of insulin sensitivity and mitochondrial homeostasis in skeletal muscle with aging.

Protein kinase C (PKC) is a family of serine/threonine kinases that play important roles in many cellular signaling events, including cell growth, differentiation, apoptosis, and hormonal responses. PKCs are classified into three major categories: conventional PKCs (α, βI, βII, γ), novel PKCs (δ, ε, ν, θ), and atypical PKCs (ζ, ι, λ) (1–3). A number of PKC isoforms have been implicated in both insulin action (4,5) and insulin resistance (6,7). Activation of conventional and novel PKCs by insulin, hyperglycemia, and lipids, especially diacylglycerol, has been shown to lead to insulin resistance (7–9). PKCδ is a member of the novel family of PKC proteins and is involved in many pathological conditions, including ischemic heart disease (10,11) and cancer (12).

PKCδ has also been implicated in insulin action and insulin resistance (4,5,13–16). While in vitro studies have suggested that PKCδ plays a positive role in insulin-stimulated glucose uptake in muscle (4,5), animal studies, especially those focusing on liver, have indicated that PKCδ is a major contributor to hepatic insulin resistance (17). In previous studies using genome-wide scanning to compare the diabetes/obesity-prone C57BL/6J (B6) mice and diabetes/obesity-resistant 129S6/Sv (129) mice, we identified PKCδ as strongly linked to the development of insulin resistance (15). Mice with liver-specific reduction in PKCδ gene expression display increased hepatic insulin sensitivity, improved glucose tolerance, and reduced hepatic lipid accumulation, while mice with liver-specific overexpression of PKCδ develop hepatic insulin resistance, fatty liver, and glucose intolerance (17). However, the contribution of muscle-derived PKCδ in the development of insulin resistance in vivo has not been explored.

Skeletal muscle is the predominant site of insulin-stimulated glucose uptake in the postprandial state. Insulin resistance in muscle is one of the characteristic features of type 2 diabetes and has been shown to exist in genetically susceptible individuals years prior to the onset of clinical diabetes (18). As noted above, in vitro studies

[1]Section of Integrative Physiology and Metabolism, Joslin Diabetes Center, Harvard Medical School, Boston, MA

[2]Novo Nordisk Foundation Center for Basic Metabolic Research, Copenhagen University, Copenhagen, Denmark

Corresponding author: C. Ronald Kahn, c.ronald.kahn@joslin.harvard.edu.

Received 12 December 2014 and accepted 17 August 2015.

This article contains Supplementary Data online at http://diabetes.diabetesjournals.org/lookup/suppl/doi:10.2337/db14-1891/-/DC1.

O.B. is currently affiliated with the Cardiovascular and Metabolic Diseases Research Unit, Pfizer, Cambridge, MA.

have suggested a positive role of PKCδ in insulin-stimulated glucose uptake performed in skeletal muscle cells (4,5). Aging is associated with many metabolic changes including lipid accumulation and the development of insulin resistance (19,20). These changes lead to increased prevalence of diabetes and metabolic syndrome beginning in middle-aged individuals and increasing thereafter. In the current study, we explored the role of PKCδ on muscle insulin sensitivity in relation to diet and age by generating mice in which the PKCδ gene has been specifically deleted in skeletal muscle using Cre-lox recombination. We found that while PKCδ does not appear to play a role in muscle insulin resistance associated with diet-induced obesity, PKCδ does play a role in the onset of insulin resistance in muscle as the mice enter middle age. Thus, PKCδ levels in muscle increase with age, and muscle-specific deletion of PKCδ improves whole-body insulin sensitivity, reverses whole-body glucose intolerance, and improves muscle insulin signaling in middle-aged mice. Hence, PKCδ is a component of insulin resistance as mice mature/age, suggesting its potential as a therapeutic target for type 2 diabetes.

RESEARCH DESIGN AND METHODS

Animals

PKCδ-floxed (control) and muscle creatine kinase–Cre transgenic (M-PKCδKO) mice have been previously described (17,21). All mice were housed in a 20–22°C temperature-controlled room on a 12-h light and dark cycle and were allowed ad libitum access to water and food. Animals were maintained on a standard chow diet (CD) containing 22% calories from fat (Mouse Diet 9F 5020; PharmaServ), or given a high-fat diet (HFD) containing 60% calories from fat (OpenSource Diet D 12492; Research Diets). All animal studies were performed according to protocols approved by the Institutional Animal Care and Use Committee (Joslin Diabetes Center).

Metabolic Studies

For the glucose tolerance test, mice were fasted overnight and injected with glucose (2 g/kg body wt i.p.). Intraperitoneal insulin tolerance tests were performed in the mice after 4 h fasting, and insulin was given (1 mU/g body wt i.p.). Glucose levels were measured in blood collected from the tail at the indicated times using Infinity glucose monitors and strips (US Diagnostics). Serum insulin levels were assessed by ELISA according to the manufacturer's recommendation (Crystal Chem).

Body Composition and Metabolic Analysis

Body composition was measured using DEXA scanning (Lunar PIXImus2 densitometer; GE Medical Systems) after anesthesia using Avertin (tribromoethanol:*tert*-amyl alcohol, 0.015 mL/g i.p.). Mice were housed individually and assessed for metabolic activities using an OPTO-M3 sensor system (Comprehensive Laboratory Animal Monitoring System [CLAMS]; Columbus Instruments, Columbus, OH). Food intake, spontaneous activity, volume of oxygen consumption, and volume of CO_2 production were measured over a 48-h light and dark cycle.

Mitochondrial Isolation and Oxygen Consumption Rate Analysis

Mitochondria were isolated and purified from hindlimb muscle using a protocol modified from one previously described (22). Briefly, 0.5 g hindlimb skeletal muscle was excised and digested in a buffer containing dispase (1 mg/g muscle weight) and trypsin (10 mg/g muscle weight) for 10 min on ice. The tissue pieces were homogenized using a Potter-Elvehjem homogenizer and centrifuged at 600*g* for 10 min at 4°C. The supernatant containing the mitochondrial fraction was filtered through cheese cloth and centrifuged at 14,000*g* for 10 min at 4°C. The pellet was resuspended and washed two more times in wash buffer (100 mmol/L KCl, 50 mmol/L Tris HCl, 1 mmol/L $MgCl_2$, 0.2 mmol/L EDTA, and 0.2 mmol/L ATP, pH 7.4) to get the final mitochondrial pellet. Isolated mitochondria were diluted in the Mitochondrial Assay Solution (70 mmol/L sucrose, 220 mmol/L mannitol, 10 mmol/L KH_2PO_4, 5 mmol/L $MgCl_2$, 2 mmol/L HEPES, 1.0 mmol/L EGTA, and 0.2% fatty acid–free BSA, pH 7.2) supplied with 10 mmol/L pyruvate/2 mmol/L malate or 40 μmol/L palmitoyl-carnitine/0.5 mmol/L malate. Oxygen consumption rate (OCR) was measured using a Seahorse Bioscience XF24 analyzer in the absence (basal) or presence (state 3) of 400 μmol/L ADP. ADP-independent respiration activity (state 4) was measured in the presence of 2 μmol/L oligomycin. Protein concentrations were measured using the Bradford method (Bio-Rad).

Hyperinsulinemic-Euglycemic Clamp

Insulin sensitivity was measured in the mice at 6 months of age by performing hyperinsulinemic-euglycemic clamp coupled with D-[3-^{3}H]glucose and ^{14}C-deoxyglucose infusions as previously described (23). Whole-body insulin sensitivity and muscle-specific glucose uptake were measured using a continuous insulin infusion dose of 5 mU/kg/min and a constant level of blood glucose at 100 mg/dL during the clamp. Whole-body insulin sensitivity was expressed as GIR, which was determined by the level of exogenous glucose infusion to maintain blood glucose levels as the initial levels during the clamp. Insulin-stimulated glucose uptake into the muscle was assessed during the final 45 min of the hyperinsulinemic-euglycemic clamp.

In Vivo Insulin Signaling, Western Blot, and Reactive Oxygen Species/Reactive Nitrogen Species Assay

After 6 h of fasting, mice were anesthetized using Avertin (240 mg/kg body wt) and injected with regular human insulin (Novolin) at the doses of either 200 units/kg body wt or 20 units/kg body wt via the inferior vena cava. Muscles were dissected 10 min after the insulin bolus and frozen in liquid nitrogen. For Western blot analysis, muscles were homogenized in RIPA buffer (Thermo Scientific) supplemented with phosphatase inhibitor and protease inhibitor cocktail (Sigma-Aldrich). Antibodies against phospho-Akt, phospho–extracellular signal–related kinase (ERK), phospho-insulin receptor (IR)β, Akt, ERK, and voltage-dependent anion channel (VDAC) were purchased from

Cell Signaling Technology. Antibodies against PKCδ, IRβ, and GAPDH were purchased from Santa Cruz Biotechnology. The phospho–insulin receptor substrate (IRS)-1 antibody was purchased from Invitrogen, antibody against IRS-1 was purchased from BD Biosciences, and antibodies against OXOPHOS proteins (mitochondrial complex I, II, and IV) were from Abcam. For muscle fractionation, cytoplasmic and membrane protein was collected from skeletal muscle using a plasma membrane protein extraction kit (ab65400; Abcam). Muscle oxidative levels were determined by a spectrofluorimetric method using the OxiSelect in vitro ROS/RNS Assay kit (STA-347; Cell Biolabs).

Ex Vivo Glucose Uptake

Muscle glucose uptake was measured as previously described (24,25). Briefly, extensor digitorum longus (EDL) and soleus muscles were dissected from 7-month-old control and M-PKCδKO mice and incubated in Krebs-Ringer bicarbonate buffer that contains 2 mmol/L pyruvate for 1 h in the presence or absence of 2.5 mU/mL insulin. Muscles were then transferred to transport solution in Krebs-Ringer bicarbonate buffer with 7 mmol/L ^{14}C-D-mannitol and 1 mmol/L [^{3}H]2-deoxyglucose (2-DG) with or without insulin. Accumulation of [^{3}H]2-DG was determined, and rates of uptake were calculated as described previously (24).

Exercise Capacity and Muscle Grip Strength Tests

Maximal exercise tolerance was measured in 7-month-old mice using a treadmill running protocol, modified from the previously described assay (26). In brief, mice were given 30 min to acclimate to the treadmill (Columbus Instruments, Columbus, OH). They then exercised at 5 m/min at 0° incline for 5 min, and after each interval (5 min) the speed was increased by 5 m/min until reaching 20 m/min with 0° incline. The slope was then increased 5 degrees every 5 min while maintaining the speed at 20 m/min until the last mouse reached the exhaustion point. Maximal exercise tolerance was determined by the cumulative amount of work (kJ) that each mouse performed, calculated as body weight (kg) × vertical distance covered (m) × 9.81. Muscle strength of the forelimbs of each mouse was measured using a Grip Strength Meter (Columbus Instruments) as described previously (27). In brief, each mouse was held from the tip of its tail and the front paws grasped the grid. The grip was released when the mouse was pulled back gently. Hindlimbs were kept free during the test. Each animal was tested three times with a 5-min break between each measurement.

Muscle Fiber Purification

Mice were perfused with saline via the left ventricle. Single tibialis anterior (TA) muscle fibers were isolated with fine forceps under a bright-field microscope after perfusion. Isolated fibers were homogenized and processed as described above, and PKCδ protein expression was measured by Western blot.

Gene Expression Analysis

Total RNA was extracted from tissues using Trizol. RNA (1 μg) was reverse transcribed using a high-capacity complementary DNA reverse transcription kit (Applied Biosystems) according to the manufacturer's instructions. Quantitative real-time PCR was performed in 5 μL of the resulting cDNA after a 10-fold dilution in the presence of the SYBR Green PCR Master Mix (Applied Biosystems) and 300 nmol/L primers. PCR reactions were run in duplicate in the ABI Prism 7700 Sequence Detection System, and Ct values were normalized to GAPDH gene levels. PKCδ primer sequence is as follows: F, 5′-CAGCCTTT CTGTGCTGTGAA-3′; R, 5′-CTGGATAACACGGCCTTCAT-3′. GAPDH primer sequence is as follows: F, 5′-TGTCGTGGAG TCTACTGGTGTCTT −3′; R, 5′-TCTCGTGGTTCACACCCATC ACAA-3′.

Statistics

Data are expressed as mean ± SEM. Differences were analyzed using an unpaired Student *t* test, one-way ANOVA, or two-way ANOVA. One-way ANOVA was followed by the Tukey multiple comparison post hoc test, and two-way ANOVA was performed using the Bonferroni multiple comparison posttest. Statistical calculations were performed using the GraphPad Prism software (GraphPad, San Diego, CA). A probability value of <0.05 was considered significantly different.

RESULTS

Muscle PKCδ Expression Increases in B6 Mice as They Age but Not in Response to HFD

Aging and obesity are two major causes of insulin resistance and diabetes (28). We first assessed whether PKCδ expression was regulated in mice by dietary insult or during aging. PKCδ protein levels in muscle increased significantly in an age-dependent manner, increasing to 165% and 170% of the 10-week-old level at 8 months and 15 months of age, respectively (Fig. 1*A*). In contrast to our previous studies, which showed increased hepatic PKCδ expression in response to HFD (17), muscles from mice challenged with an HFD for 10 weeks displayed a reduction in PKCδ protein levels by 50% (Fig. 1*B* and *C*).

Mice With Muscle-Specific PKCδ Deletion Display Improved Insulin Signaling at 10 Weeks of Age

Previous in vitro studies suggested an important role for PKCδ in insulin-stimulated glucose uptake in muscle (4,5), while in vivo studies indicated a role for PKCδ in liver leading to insulin resistance (14,16,17). To assess the true metabolic role of PKCδ in muscle in vivo, we generated a mouse in which the PKCδ gene was deleted specifically in muscle by breeding mice in which exon 2 of PKCδ was flanked with loxP sites with mice carrying the Cre recombinase gene driven by the muscle creatine kinase promoter (17,29). The resultant M-PKCδKO mice exhibited remarkable decreases of PKCδ mRNA levels in TA (74%), quadriceps (82.6%), gastrocnemius (79%), and EDL (65%) muscles (all $P < 0.05$) (Fig. 2*A*). Likewise, a 70% reduction of PKCδ protein levels was observed in TA muscle fibers purified from M-PKCδKO mice (Fig. 2*B*). At 10 weeks of age, M-PKCδKO mice did not show differences in body

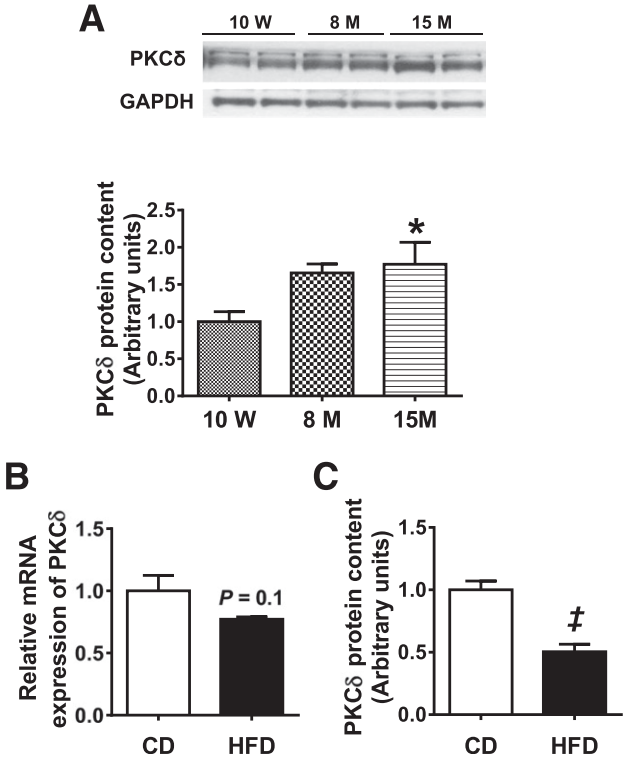

Figure 1—Effect of aging and HFD on PKCδ muscle expression in wild-type B6 mice. *A*: PKCδ protein content in triceps muscle of 10-week-old, 8-month-old, and 15-month-old wild-type B6 mice as measured by Western blot analysis (n = 8 per group). PKCδ mRNA expression (*B*) and protein content (*C*) in TA muscle of 3-month-old wild-type B6 mice fed either a CD or an HFD for 10 weeks. A representative Western blot is shown in Fig. 3*C*. Data are mean ± SEM. n = 8. *P < 0.05 vs. 10 weeks by one-way ANOVA; ‡P < 0.05 vs. CD by Student t test. M, month; W, week.

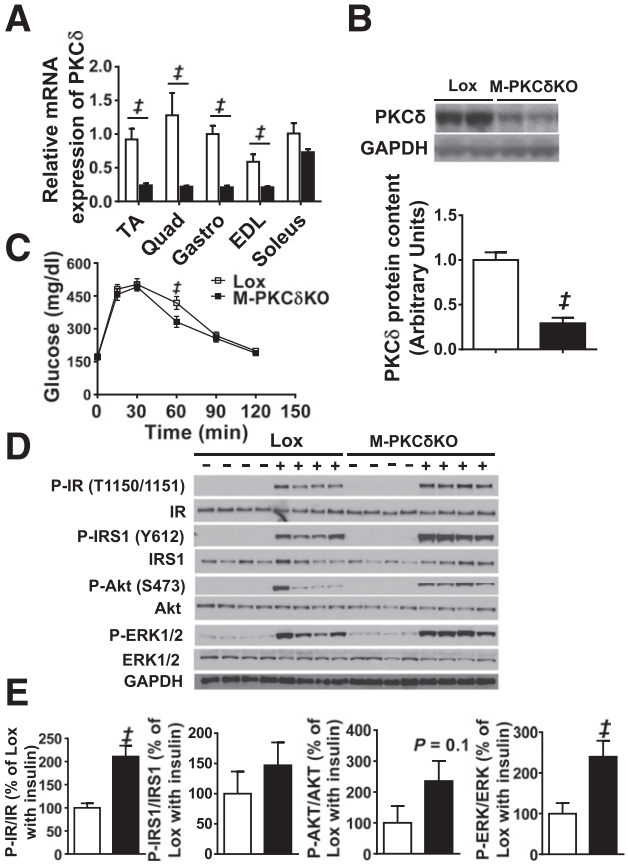

Figure 2—Glucose tolerance and muscle insulin signaling are normal in muscle-specific PKCδ knockout mice at 10 weeks of age. *A*: PKCδ mRNA expression in TA, quadriceps (Quad), gastrocnemius (Gastro), EDL, and soleus muscles from Lox and M-PKCδKO mice. *B*: Representative Western blots and densitometric quantification of PKCδ in the purified TA muscle fibers of Lox and M-PKCδKO mice with quantification below. *C*: Intraperitoneal glucose tolerance tests were performed in Lox and M-PKCδKO mice. *D*: Western blot analysis of insulin signaling pathway in skeletal muscle of Lox and M-PKCδKO mice after insulin injection (20 units/kg body wt i.v.). *E*: Densitometric analysis of IR, IRS-1, AKT, and EKR phosphorylation from *D* after insulin stimulation. □, Lox mice; ■, M-PKCδKO mice. Data are means ± SEM. n = 6–8 per group in panels *A*–*C*, and n = 4 per group for panels *D* and *E*. ‡P < 0.05 by Student t test.

weight or body composition (i.e., fat and lean mass) as assessed by DEXA compared with control littermates (Supplementary Fig. 1*A*). Furthermore, at sacrifice, no differences in body weight or muscle weights were observed (data not shown). Muscle fiber size (data not shown) and gene expression of myosin—proteins that define fiber type—remained unchanged (Supplementary Fig. 1*B*). Intraperitoneal glucose tolerance tests (GTTs) performed at 10 weeks of age revealed no difference between the M-PKCδKO and control mice with the exception of a small, but significant, decrease in glucose levels at 60 min in M-PKCδKO mice (Fig. 2*C* and Supplementary Fig. 1*C*). Likewise, intraperitoneal insulin tolerance tests demonstrated no difference in the insulin-mediated reduction of glucose levels between knockout and control mice (Supplementary Fig. 1*D*), and plasma insulin levels in both the fasted and fed states were unchanged (Supplementary Fig. 1*E*).

However, insulin signaling, especially at low insulin doses, was improved in M-PKCδKO mice. Thus, after injection of insulin (20 units/kg body wt) into the vena cava of 10-week-old mice, phosphorylation of IR in TA muscle was increased by 2.1-fold in M-PKCδKO mice compared with control (Fig. 2*D* and E). Likewise, insulin-stimulated phosphorylation of AKT and ERK was increased by 1.5-fold and 1.4-fold in M-PKCδKO mice compared with controls. Interestingly, when insulin was injected at a higher dose (200 units/kg body wt), no difference was observed between control and M-PKCδKO mice, suggesting saturation of insulin receptor signaling (Supplementary Fig. 1*F* and *G*) at the high dose.

HFD-Induced Glucose Intolerance and Muscle Insulin Resistance Are Not Prevented by PKCδ Deletion in Muscle

Previous studies have shown that PKCδ is increased in the liver of HFD-induced obese mice and that PKCδ plays an important role in liver in HFD-induced insulin resistance (17). To assess the role of PKCδ in muscle on HFD-induced insulin resistance, we placed 5-week-old M-PKCδKO and control mice on either an HFD (60% fat by calories) or

CD (22% fat by calories) and followed them for 10 weeks. During this time, control mice on CD gained 52% above their starting body weight, and those on HFD gained almost twice as much (Fig. 3*A*). Body composition as assessed by DEXA at the end of the diet period revealed that the M-PKCδKO mice on CD had a tendency to have a greater lean mass than controls (Supplementary Fig. 2*A*), but this did not quite reach statistical significance. After 10 weeks of HFD, both control and M-PKCδKO mice had a similar twofold increase in fat mass (Supplementary Fig. 2*B*).

To determine whether this difference in body weight and composition was associated with a change in energy balance, we monitored the metabolic activities of the M-PKCδKO and control mice using metabolic cages. M-PKCδKO mice displayed food intake similar to that of control mice (Supplementary Fig. 2*C*) but showed a trend toward increased spontaneous activity during the light phase (Supplementary Fig. 2*D*). The OCR and respiratory exchange ratio were not different between M-PKCδKO and control mice (Supplementary Fig. 2*E* and *F*). Despite the higher spontaneous activity, M-PKCδKO mice showed no difference in the expression of genes that mark muscle fiber type (myosin IIa, myosin IIx, and myosin IIb) or differentiation (myoD1 and myf5) on both CD and HFD (Supplementary Fig. 2*G*).

Fasting plasma glucose levels were unchanged between control and M-PKCδKO mice on either CD or HFD (Supplementary Fig. 3*A*). Control mice fed an HFD for 10 weeks showed a twofold increase in plasma insulin levels, and insulin levels were further increased by ~40% in M-PKCδKO mice on both chow and HFD diet compared with control (Fig. 3*B*). Both control and M-PKCδKO mice showed impaired glucose tolerance on HFD (Supplementary Fig. 3*B*) and higher levels of glucose throughout the insulin tolerance test (Supplementary Fig. 3*C*) with no differences between control and M-PKCδKO mice. As expected, HFD challenge in control mice resulted in reduced muscle insulin signaling with decreased levels of IRS-1 tyrosine phosphorylation and AKT serine phosphorylation (Fig. 3*C*), even when stimulated with insulin at a dose of 200 units/kg body wt. The reduction in insulin signaling, however, was not affected by PKCδ deletion in muscle. Consistent with the data shown in Fig. 1, Western blot analysis revealed that PKCδ expression in muscle was reduced by HFD treatment by 50% in control mice. Since PKCδ activation is associated with translocation to cell membranes (30), we determined the amount of PKCδ protein associated with the membrane fraction in muscle of control and M-PKCδKO mice on both diets. The ratio of membrane to cytosolic fraction of PKCδ was increased by 54% on HFD in control mice, consistent with the increased activation of PKCδ by HFD. Compared with control, M-PKCδKO mice demonstrated a 56% decrease in the ratio of membrane to cytosolic fraction of PKCδ on CD and a 70% decrease in the ratio on HFD (Fig. 3*D*). No differences were found in the levels of the reactive oxygen species (ROS) and reactive nitrogen species (RNS) between M-PKCδKO and control mice on CD or HFD (Supplementary Fig. 3*D*).

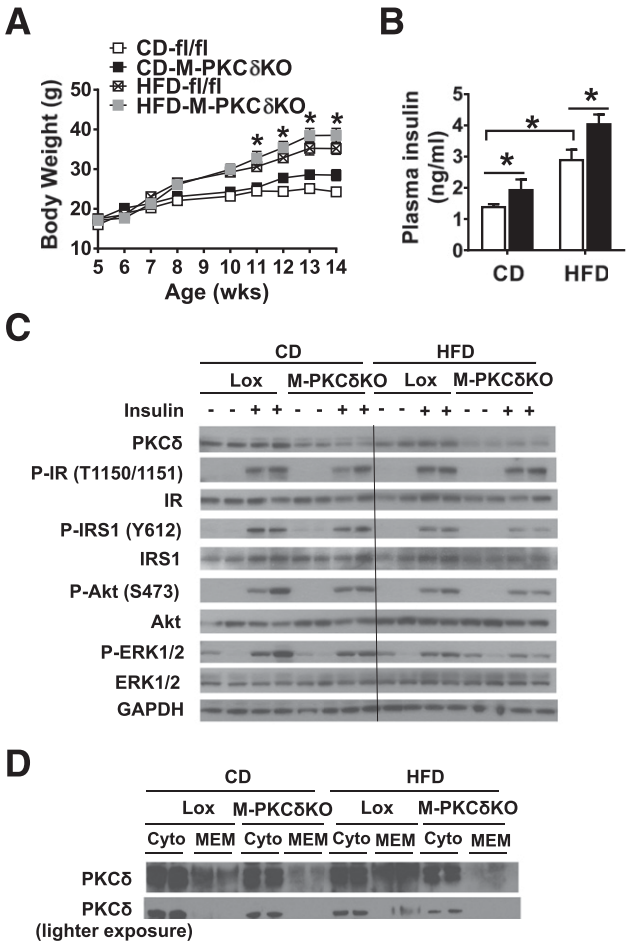

Figure 3— Muscle-specific knockout of PKCδ does not alleviate HFD-induced muscle insulin resistance. *A*: Body weight changes of Lox and M-PKCδKO mice fed either a CD or an HFD from 5 to 16 weeks (wks) of age (n = 10 per group). *B*: Insulin levels were measured in 4-month-old Lox and M-PKCδKO mice fed either a CD or an HFD (n = 6–8 per group). *C*: Western blot analysis of insulin signaling in TA muscle of Lox and M-PKCδKO after insulin injection (200 units/kg body wt i.v.). *D*: Western blot of PKCδ protein in cytoplasmic (cyto) and membrane (MEM) fractions of gastrocnemius muscle from Lox and M-PKCδKO mice fed either a CD or an HFD. □, Lox mice; ■, M-PKCδKO mice. Data are means ± SEM. *P < 0.05 by two-way ANOVA in *A* (CD-treated control vs. HFD-treated control mice) and *B*.

Insulin Sensitivity and Glucose Tolerance Are Improved in M-PKCδKO Mice at 6–7 Months of Age

This increase was associated with a trend toward increased uptake of ^{14}C-deoxyglucose in the skeletal muscles (TA, EDL, soleus, and quadriceps) of the M-PKCδKO mice (Fig. 4*B*). When insulin-stimulated glucose uptake was assessed ex vivo in soleus and EDL muscle strips, the M-PKCδKO mice also displayed a trend to increased glucose uptake, with 44–47% increases of insulin-stimulated [^{3}H]2-DG uptake into isolated EDL and soleus muscles (Supplementary Fig. 4*A* and Fig. 4*C*). This was associated with significant 21–25% reductions in glucose levels at 60 and 90 min during intraperitoneal GTT in 7-month-old

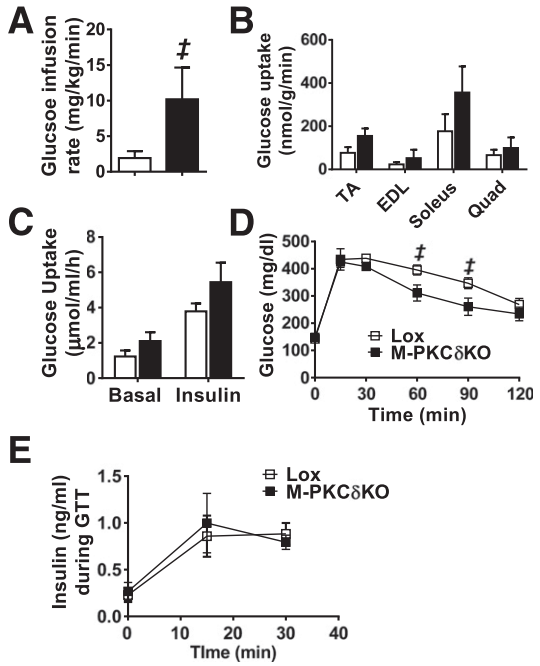

Figure 4—Muscle-specific knockout of PKCδ improves whole-body insulin sensitivity and glucose tolerance at 6 to 7 months of age. GIR (*A*) and insulin-stimulated ^{14}C-deoxyglucose uptake (*B*) were measured during hyperinsulinemic-euglycemic clamps in 6-month-old M-PKCδKO mice (n = 3–7). *C*: Rates of [^{3}H]2-DG uptake into soleus muscles in the presence or absence of 2.5 mU/mL insulin (n = 4–5). Intraperitoneal GTT (*D*), and insulin secretion during GTT (*E*) at 0, 15, and 30 min (n = 5). □, Lox mice; ■, M-PKCδKO mice. Data are mean ± SEM. ‡P < 0.05 by Student t test.

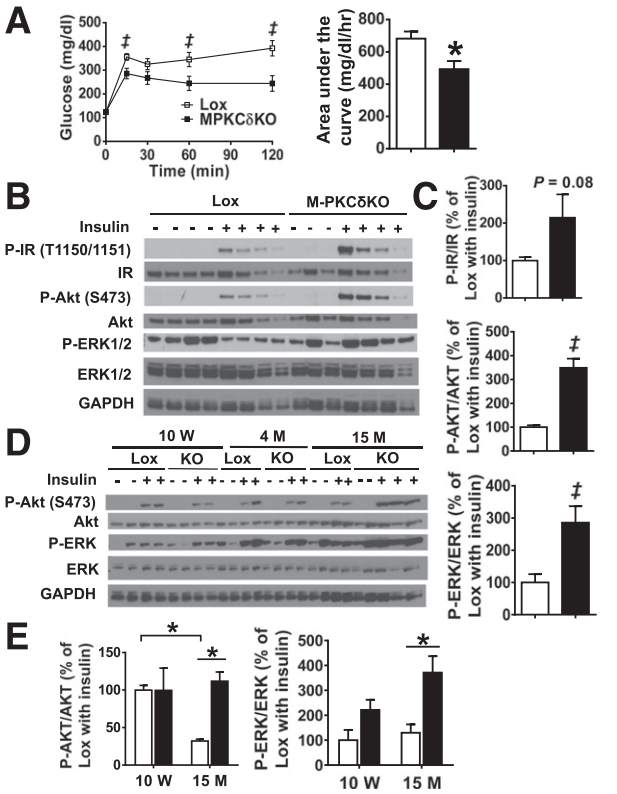

Figure 5—Glucose tolerance and muscle insulin signaling are improved in M-PKCδKO mice at 15 months of age. *A*: Intraperitoneal GTTs were performed in 15-month-old Lox and M-PKCδKO mice (n = 12 per group), and area under the curve was measured. *B*: Insulin signaling was analyzed in TA muscle of 15-month-old Lox and M-PKCδKO mice by Western blot after insulin injection (200 units/kg body wt i.v.). *C*: Insulin-stimulated phosphorylation of the insulin receptor, AKT, and ERK after insulin stimulation were quantified by densitometric analysis. *D*: Representative Western blot of insulin signaling from TA muscles of Lox and M-PKCδKO mice at 10 week, 4 months, and 15 months of age. *E*: Densitometric analysis of insulin-stimulated AKT and ERK phosphorylation at 10 weeks and 15 months of age. □, Lox mice; ■, M-PKCδKO mice. Data are mean ± SEM. ‡P < 0.05 by Student t test; *P < 0.05 by two-way ANOVA. M, month; W, week.

M-PKCδKO mice (Fig. 4*D* and Supplementary Fig. 4*B*). Insulin secretion at 0, 15, and 30 min during GTT was unchanged in M-PKCδKO mice (Fig. 4*E*), and intraperitoneal insulin tolerance tests demonstrated no difference in the insulin-mediated reduction of glucose levels between M-PKCδKO and control mice (Supplementary Fig. 4*C*). Assessment of maximal exercise capacity and forelimb grip strength revealed no differences between age-matched control and M-PKCδKO mice (Supplementary Fig. 5*A* and *B*).

Glucose Intolerance and Insulin Resistance Are Alleviated by Muscle-Specific PKCδ Deletion at 15 Months of Age

At 15 months of age, muscle-specific PKCδ deletion led to a marked improvement of glucose tolerance with a 28% decrease in AUC ($P < 0.05$) (Fig. 5*A*). As in the younger animals, this improved glucose tolerance was not associated with changes in serum insulin levels in the fasted or fed state (Supplementary Fig. 7*A*). To determine whether the improvement of glucose tolerance was related to improved muscle insulin sensitivity in old M-PKCδKO mice, we measured insulin signaling in the TA muscle from older control and M-PKCδKO mice at 15 months of age. At this age, after high-dose (200 units/kg body wt i.v.) insulin injection, phosphorylation of AKT on serine 473 was increased by 3.5-fold, with parallel changes in ERK phosphorylation in M-PKCδKO muscle compared with controls (Fig. 5*B* and *C*).

To determine whether deletion of PKCδ in muscle could prevent the age-related decline in insulin signaling, we compared insulin-medicated AKT and ERK phosphorylation in muscle from control and M-PKCδKO mice at different ages. Compared with 10-week-old mice, control mice at 15 months of age exhibited a 68% reduction in insulin-stimulated AKT serine 473 phosphorylation, which was prevented in M-PKCδKO mice (Fig. 5*D* and *E*). This correlated with increased protein levels of PKCδ in muscle as the mice aged (Supplementary Fig. 6). Thus, compared with control mice, M-PKCδKO mice exhibited age-dependent decreases in PKCδ protein levels, decreasing by 30% and 75% at 4 and 15 months of age,

respectively. The residual protein levels PKCδ may represent an incomplete rearrangement of the floxed alleles in a small subset of myofibers or, more likely, the presence of other cells types such as satellite cells, adipocytes, endothelial cells, and fibroblasts (21). Indeed, isolated endothelial cells exhibited 15-fold higher levels of PKCδ mRNA expression compared with skeletal muscle (Supplementary Fig. 6*B* and *C*) when normalized to GAPDH. This high level of PKCδ expression in endothelial cells likely accounts for the residual expression of PKCδ observed in both the whole tissue lysates and the isolated muscle fibers.

Impact of Muscle-Specific PKCδ Deletion on Body Composition and Energy Expenditure at 15 Months of Age

Metabolic assessment was performed in M-PKCδKO and control mice at 15 months of age. While the total body and muscle weight did not change (data not shown), DEXA analysis at this age revealed that M-PKCδKO mice had 10% less total fat and 9% less visceral fat compared with control mice (Fig. 6*A* and *B*). Furthermore, M-PKCδKO mice had a 16.5% increase in the ratio of lean mass to fat mass compared with control mice (Fig. 6*C*).

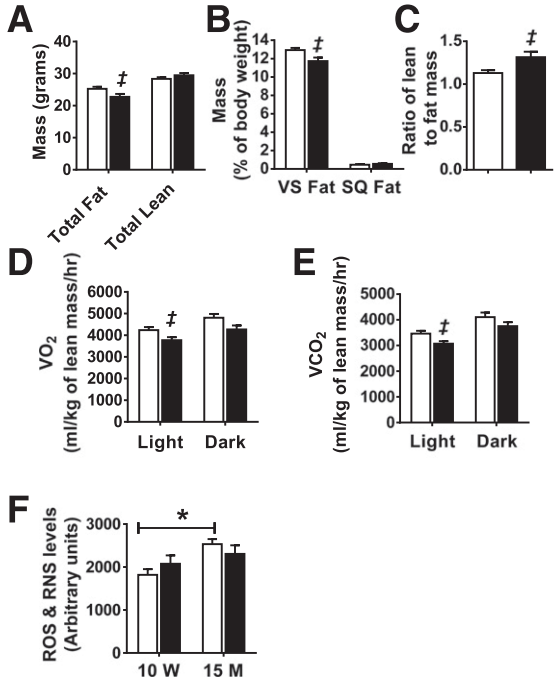

Figure 6—Impact of muscle-specific deletion of PKCδ on body composition and energy expenditure at 15 months of age. Total fat and lean mass (*A*), percentage of visceral fat (VS) and subcutaneous fat (SQ) per body weight (*B*), and ratio of lean mass to fat mass (*C*) were assessed by DEXA in 15-month-old Lox and M-PKCδKO mice (n = 12 per group). Oxygen consumption (*D*) and CO_2 production (*E*) measured in Lox and M-PKCδKO mice over 48 h in CLAMS metabolic cages (n = 12 per group). *F*: ROS and RNS were measured in TA muscles of Lox and M-PKCδKO mice at 10 weeks and 15 months of age. □, control mice; ■, M-PKCδKO mice. Data are mean ± SEM. ‡$P < 0.05$ by Student t test. *$P < 0.05$ by two-way ANOVA. M, month; hr, hour; W, week.

Gene expression of muscle fiber type markers and markers of differentiation indicated that there was no change in the characteristics of muscle from older M-PKCδKO mice (Supplementary Fig. 7*B*). CLAMS metabolic cage analysis revealed that while M-PKCδKO mice showed food intake and activity similar to those of control mice (Supplementary Fig. 7*C* and *D*), oxygen consumption and CO_2 production normalized to lean body mass in older M-PKCδKO mice were reduced significantly by 10% and 11%, respectively, during the light cycle. A similar trend was also observed during the dark cycle (Fig. 6*D* and *E*). Respiratory exchange ratio was not different between the two genotypes (Supplementary Fig. 7*E*).

To investigate the mechanism by which muscle-specific PKCδ deletion leads to decreased oxygen consumption, we isolated mitochondria from 15-month-old M-PKCδKO and control mice and measured their metabolic capacity using different substrates in the absence (basal) or presence of ADP (state 3). In the presence of pyruvate/malate (PDH and complex I substrate), the addition of ADP increased the OCR by 1.6-fold over basal in mitochondria isolated from older control mice, and mitochondria of age-matched M-PKCδKO mice displayed a similar change (Supplementary Fig. 7*F*). Likewise, in the presence of palmitoyl-carnitine/malate (β-oxidation substrate), both control and M-PKCδKO mice displayed a 2.2-fold increase in the OCR in state 3 compared with the basal state (Supplementary Fig. 7*G*). The respiratory control ratio (state 3/state 4), an index of mitochondrial coupling, was also similar between control and M-PKCδKO mice in the presence of either pyruvate/malate or palmitoyl-carnitine/malate (Supplementary Fig. 7*H*). Protein levels of the VDAC were decreased by 80% and levels of complex I subunit also trended to be decreased in 15-month-old M-PKCδKO mice compared with control littermates (Supplementary Fig. 8*A* and *B*). Compared with 10-week-old mice, the ROS and RNS levels in muscle were significantly increased by 19% in 15-month-old control mice (Fig. 6*F*). Together, these data suggest a role for PKCδ in the regulation of mitochondrial homeostasis at older age.

DISCUSSION

We previously demonstrated an important role of PKCδ in the regulation of hepatic insulin sensitivity and hepatosteatosis in both mice and humans (17). Indeed, PKCδ levels in liver are higher in strains of mice that are susceptible to diet-induced obesity and insulin resistance. Overexpression of PKCδ in liver of mice increases insulin resistance, and liver-specific knockout of PKCδ in mice challenged with HFD improves insulin sensitivity and glucose tolerance. On the other hand, previous studies with myoblasts and myotubes in vitro indicate that PKCδ may play a different role in muscle serving as a positive regulator of insulin signaling

(4,5,31). Moreover, overexpression of PKCδ in primary muscle cells has been shown to increase GLUT4 translocation and glucose uptake in the basal state, and pharmacological inhibition of PKCδ caused downregulation of insulin-induced GLUT4 translocation and glucose uptake (5). In cultured muscle cells, insulin stimulation has also been shown to lead to a direct association of PKCδ with the insulin receptor, with enhanced insulin-induced tyrosine phosphorylation and insulin receptor internalization (31). In *Psammomys obesus,* exercise also increases PKCδ levels in muscle and insulin receptor phosphorylation (32,33).

In the current study, we investigated the role of PKCδ in skeletal muscle insulin action and whole-body insulin sensitivity by creating an M-PKCδKO mouse. We found that at a young age, muscle insulin signaling was improved in M-PKCδKO mice when stimulated with a low dose of insulin of 20 units/kg body wt but was not changed at maximal doses (200 units/kg body wt), consistent with improved insulin sensitivity with no change in maximal response. Despite the increased signaling in M-PKCδKO muscle at the lower dose, decreased PKCδ level in muscle had no effect on whole-body glucose tolerance in mice placed on either CD or HFD. However, at 6 months of age M-PKCδKO mice demonstrated an improvement in whole-body insulin sensitivity as measured during a hyperinsulinemic-euglycemic clamp. At 15 months of age, muscle-specific deletion of PKCδ in mice improved muscle insulin signaling and resulted in a significant improvement in glucose tolerance. The improvement in insulin sensitivity and glucose tolerance was also accompanied by a shift toward a "leaner" body composition in the older M-PKCδKO mice with less fat, especially visceral fat, and a higher ratio of lean to fat mass. Since the accumulation of visceral fat is an important contributor to the development of diabetes and insulin resistance (18,28), it is possible that the decreased visceral fat observed in old M-PKCδKO mice plays a role in the improved insulin sensitivity and glucose tolerance. These data also suggest a crosstalk between muscle and fat, similar to that previously observed when the insulin receptor was deleted from muscle (MIRKO mouse) but in the opposite direction; i.e., in MIRKO mice, fat mass is increased (34). One reason for the different responses observed in M-PKCδKO mice at different ages is the increase in PKCδ expression in muscle as the mice progressed in age. Indeed, PKCδ protein levels in muscle increase by 70% as the mice mature from 10 weeks to 15 months of age. Many previous in vitro studies have shown that upon exposure to ROS, PKCδ is upregulated and activated to initiate important cellular responses (35,36). Indeed, at 15 months of age mice demonstrated a 19% increase of ROS/RNS levels in skeletal muscle compared with younger cohorts, suggesting that the accumulation of ROS during the aging process may contribute to the increased levels of PKCδ.

Previous studies have shown that PKCδ plays important roles in the regulation of mitochondrial mass and mitochondrial metabolism (37–39). Indeed, markers of mitochondrial mass, such as VDAC protein and mitochondrial complex I protein, were decreased in 15-month-old M-PKCδKO mice. M-PKCδKO mice also displayed a 10% reduction in oxygen consumption at the whole-body level compared with controls. To see whether loss of PKCδ impairs mitochondrial function, we determined OCRs in isolated mitochondria from M-PKCδKO and control mice at 15 months of age. Surprisingly we observed no differences in basal or ADP-dependent mitochondrial oxidative capacity when using two different substrates and normalized to mitochondrial protein. These data suggest PKCδ may play an important role in the maintenance of mitochondrial mass in skeletal muscle but does not have as great an impact on mitochondrial function.

We previously showed that liver-specific reduction of PKCδ in HFD-treated obese mice improved glucose tolerance and insulin sensitivity by decreasing IRS-1 serine phosphorylation and increasing Akt phosphorylation (17). We hypothesized that similar mechanisms might contribute to HFD-induced insulin resistance in muscle and that muscle-specific PKCδ deletion may rescue HFD-induced insulin resistance. Indeed, several previous studies have shown that diacylglycerol accumulation in muscle can activate novel PKCs, such as PKCθ, and impair muscle insulin action (40). However, our results show that in contrast to liver-specific PKCδ deletion, PKCδ deletion in muscle is not sufficient to rescue the HFD-induced glucose intolerance and muscle insulin resistance. These opposite observations may be explained by the opposing expression patterns of PKCδ in the two tissues when exposed to HFD. Hepatic PKCδ expression was increased by >50% in the HFD-treated B6 mice compared with the CD group. However, muscle PKCδ expression was decreased by 50% in mice placed on HFD compared with those on CD, indicating differences in PKCδ regulation in these tissues. While the mechanism of the HFD-induced differences in PKCδ expression in liver and muscle is unclear, activation of other PKC isoforms in muscle, such as PKCθ and ε, may contribute to the impairment of insulin signaling in muscle and overcome the protective effect of PKCδ deletion in the muscle of mice with diet-induced obesity (41–43).

In summary, the role of PKCδ in muscle is different depending on the etiology of insulin resistance. While the role of PKCδ in elderly animals remains to be determined, PKCδ levels are increased in skeletal muscle of middle-aged mice, and muscle-specific deletion of PKCδ improved the middle-age–related decline in glucose tolerance and whole-body insulin resistance. It also improved the ratio of lean to fat mass. In HFD-induced obesity, PKCδ levels were decreased in skeletal muscle, and deletion of PKCδ did not rescue HFD-induced insulin resistance and glucose intolerance. The distinct pattern of regulation in muscle and liver sheds new light on how PKCδ functions

in different insulin-responsive tissues and the therapeutic potential of PKCδ as a target for the tissue-specific improvement in insulin resistance.

Acknowledgments. The authors thank Graham Smyth for assistance with the animal care, Christian Doherty and Mike Hirshman from Laurie J. Goodyear's laboratory for assistance with the ex vivo 2-DG glucose uptake assay, Hans P.M.M. Lauritzen for assistance with the muscle fiber purification, and Erica P. Homan for assistance with the proofreading.

Funding. This work was supported by National Institutes of Health (NIH) grant R01-DK-033201 and Joslin Diabetes Research Center grant DK-036836. B.T.O. was also funded by a K08 Training award from the National Institute of Diabetes and Digestive and Kidney Diseases of the NIH (K08-DK-100543).

Duality of Interest. No potential conflicts of interest relevant to this article were reported.

Author Contributions. M.L. generated data and wrote the manuscript. S.G.V. and B.T.O. reviewed the manuscript and generated data. O.B. initiated the project and reviewed and edited the manuscript. C.R.K. oversaw the project, contributed to discussion, and helped write the manuscript. C.R.K. is the guarantor of this work and, as such, had full access to all the data in the study and takes responsibility for the integrity of the data and the accuracy of the data analysis.

References

1. Brand C, Horovitz-Fried M, Inbar A, Tamar-Brutman-Barazani, Brodie C, Sampson SR. Insulin stimulation of PKCδ triggers its rapid degradation via the ubiquitin-proteasome pathway. Biochim Biophys Acta 2010;1803:1265–1275
2. Turban S, Hajduch E. Protein kinase C isoforms: mediators of reactive lipid metabolites in the development of insulin resistance. FEBS Letters 2011;585: 269–274
3. Schmitz-Peiffer C, Biden TJ. Protein kinase C function in muscle, liver, and β-cells and its therapeutic implications for type 2 diabetes. Diabetes 2008;57: 1774–1783
4. Jacob AI, Horovitz-Fried M, Aga-Mizrachi S, et al. The regulatory domain of protein kinase C delta positively regulates insulin receptor signaling. J Mol Endocrinol 2010;44:155–169
5. Braiman L, Alt A, Kuroki T, et al. Protein kinase Cdelta mediates insulin-induced glucose transport in primary cultures of rat skeletal muscle. Mol Endocrinol 1999;13:2002–2012
6. Schmitz-Peiffer C. Signalling aspects of insulin resistance in skeletal muscle: mechanisms induced by lipid oversupply. Cell Signal 2000;12:583–594
7. Schmitz-Peiffer C. Protein kinase C and lipid-induced insulin resistance in skeletal muscle. Ann N Y Acad Sci 2002;967:146–157
8. Itani SI, Ruderman NB, Schmieder F, Boden G. Lipid-induced insulin resistance in human muscle is associated with changes in diacylglycerol, protein kinase C, and IkappaB-alpha. Diabetes 2002;51:2005–2011
9. Griffin ME, Marcucci MJ, Cline GW, et al. Free fatty acid-induced insulin resistance is associated with activation of protein kinase C theta and alterations in the insulin signaling cascade. Diabetes 1999;48:1270–1274
10. Ishii H, Koya D, King GL. Protein kinase C activation and its role in the development of vascular complications in diabetes mellitus. J Mol Med (Berl) 1998;76:21–31
11. Xia P, Aiello LP, Ishii H, et al. Characterization of vascular endothelial growth factor's effect on the activation of protein kinase C, its isoforms, and endothelial cell growth. J Clin Invest 1996;98:2018–2026
12. Kim J, Koyanagi T, Mochly-Rosen D. PKCδ activation mediates angiogenesis via NADPH oxidase activity in PC-3 prostate cancer cells. Prostate 2011;71: 946–954
13. Kellerer M, Mushack J, Seffer E, Mischak H, Ullrich A, Häring HU. Protein kinase C isoforms alpha, delta and theta require insulin receptor substrate-1 to inhibit the tyrosine kinase activity of the insulin receptor in human kidney embryonic cells (HEK 293 cells). Diabetologia 1998;41:833–838
14. Greene MW, Burrington CM, Luo Y, Ruhoff MS, Lynch DT, Chaithongdi N. PKCδ is activated in the liver of obese Zucker rats and mediates diet-induced whole body insulin resistance and hepatocyte cellular insulin resistance. J Nutr Biochem 2014;25:281–288
15. Almind K, Kahn CR. Genetic determinants of energy expenditure and insulin resistance in diet-induced obesity in mice. Diabetes 2004;53:3274–3285
16. Zhang J, Burrington CM, Davenport SK, et al. PKCδ regulates hepatic triglyceride accumulation and insulin signaling in Lepr(db/db) mice. Biochem Biophys Res Commun 2014;450:1619–1625
17. Bezy O, Tran TT, Pihlajamäki J, et al. PKCδ regulates hepatic insulin sensitivity and hepatosteatosis in mice and humans. J Clin Invest 2011;121:2504–2517
18. DeFronzo RA, Tripathy D. Skeletal muscle insulin resistance is the primary defect in type 2 diabetes. Diabetes Care 2009;32(Suppl. 2):S157–S163
19. Koonen DP, Sung MM, Kao CK, et al. Alterations in skeletal muscle fatty acid handling predisposes middle-aged mice to diet-induced insulin resistance. Diabetes 2010;59:1366–1375
20. Cheng A, Morsch M, Murata Y, Ghazanfari N, Reddel SW, Phillips WD. Sequence of age-associated changes to the mouse neuromuscular junction and the protective effects of voluntary exercise. PLoS One 2013;8:e67970
21. Brüning JC, Michael MD, Winnay JN, et al. A muscle-specific insulin receptor knockout exhibits features of the metabolic syndrome of NIDDM without altering glucose tolerance. Mol Cell 1998;2:559–569
22. Mansouri A, Muller FL, Liu Y, et al. Alterations in mitochondrial function, hydrogen peroxide release and oxidative damage in mouse hind-limb skeletal muscle during aging. Mech Ageing Dev 2006;127:298–306
23. Norris AW, Chen L, Fisher SJ, et al. Muscle-specific PPARgamma-deficient mice develop increased adiposity and insulin resistance but respond to thiazolidinediones. J Clin Invest 2003;112:608–618
24. Hayashi T, Hirshman MF, Kurth EJ, Winder WW, Goodyear LJ. Evidence for 5′ AMP-activated protein kinase mediation of the effect of muscle contraction on glucose transport. Diabetes 1998;47:1369–1373
25. Fujii N, Jessen N, Goodyear LJ. AMP-activated protein kinase and the regulation of glucose transport. Am J Physiol Endocrinol Metab 2006;291:E867–E877
26. Fewell JG, Osinska H, Klevitsky R, et al. A treadmill exercise regimen for identifying cardiovascular phenotypes in transgenic mice. Am J Physiol 1997; 273:H1595–H1605
27. Nalbandian A, Nguyen C, Katheria V, et al. Exercise training reverses skeletal muscle atrophy in an experimental model of VCP disease. PLoS One 2013;8:e76187
28. Park YW, Zhu S, Palaniappan L, Heshka S, Carnethon MR, Heymsfield SB. The metabolic syndrome: prevalence and associated risk factor findings in the US population from the Third National Health and Nutrition Examination Survey, 1988-1994. Arch Intern Med 2003;163:427–436
29. Johnson JE, Wold BJ, Hauschka SD. Muscle creatine kinase sequence elements regulating skeletal and cardiac muscle expression in transgenic mice. Mol Cell Biol 1989;9:3393–3399
30. Azzi A, Boscoboinik D, Hensey C. The protein kinase C family. Eur J Biochem 1992;208:547–557
31. Braiman L, Alt A, Kuroki T, et al. Insulin induces specific interaction between insulin receptor and protein kinase C delta in primary cultured skeletal muscle. Mol Endocrinol 2001;15:565–574
32. Heled Y, Shapiro Y, Shani Y, et al. Physical exercise enhances protein kinase C delta activity and insulin receptor tyrosine phosphorylation in diabetes-prone psammomys obesus. Metabolism 2003;52:1028–1033
33. Heled Y, Shapiro Y, Shani Y, et al. Physical exercise prevents the development of type 2 diabetes mellitus in Psammomys obesus. Am J Physiol Endocrinol Metab 2002;282:E370–E375
34. Kim JK, Michael MD, Previs SF, et al. Redistribution of substrates to adipose tissue promotes obesity in mice with selective insulin resistance in muscle. J Clin Invest 2000;105:1791–1797

35. Kanthasamy AG, Kitazawa M, Kanthasamy A, Anantharam V. Role of proteolytic activation of protein kinase Cdelta in oxidative stress-induced apoptosis. Antioxid Redox Signal 2003;5:609–620
36. Yamaguchi T, Miki Y, Yoshida K. Protein kinase C delta activates IkappaB-kinase alpha to induce the p53 tumor suppressor in response to oxidative stress. Cell Signal 2007;19:2088–2097
37. Basu A. Involvement of protein kinase C-delta in DNA damage-induced apoptosis. J Cell Mol Med 2003;7:341–350
38. Mayr M, Chung YL, Mayr U, et al. Loss of PKC-delta alters cardiac metabolism. Am J Physiol Heart Circ Physiol 2004;287:H937–H945
39. Lee CF, Chen YC, Liu CY, Wei YH. Involvement of protein kinase C delta in the alteration of mitochondrial mass in human cells under oxidative stress. Free Radic Biol Med 2006;40:2136–2146
40. Kikkawa U, Matsuzaki H, Yamamoto T. Protein kinase C delta (PKC delta): activation mechanisms and functions. J Biochem 2002;132:831–839
41. Schmitz-Peiffer C, Browne CL, Oakes ND, et al. Alterations in the expression and cellular localization of protein kinase C isozymes epsilon and theta are associated with insulin resistance in skeletal muscle of the high-fat-fed rat. Diabetes 1997;46:169–178
42. Qu X, Seale JP, Donnelly R. Tissue and isoform-selective activation of protein kinase C in insulin-resistant obese Zucker rats - effects of feeding. J Endocrinol 1999;162:207–214
43. Ikeda Y, Olsen GS, Ziv E, et al. Cellular mechanism of nutritionally induced insulin resistance in Psammomys obesus: overexpression of protein kinase Cepsilon in skeletal muscle precedes the onset of hyperinsulinemia and hyperglycemia. Diabetes 2001;50:584–592